

Asymmetric Hysteresis Loops, Leakage Current and Capacitance Voltage Behaviors in Ferroelectric PZT Films Deposited on a Pt/Al₂O₃/SiO₂/Si Substrate by MOCVD method with a vapor-deposited Gold Top Electrode

Masruroh and Masayuki Toda

Abstract—The polarization-voltage (P-V), leakage currents density (J-V) characteristics and the C-V characteristics were investigated on the ferroelectric PZT films deposited on Pt/Al₂O₃/SiO₂/Si substrate with a vapor-deposited gold top electrode. The P-V hysteresis loops the J-V characteristics and the C-V characteristics were measured after performing a rapid thermal annealing (RTA) process. A ferroelectric test system (Precision LC Radiant Technology) was used to measure their electrical properties with a 90-nm PZT thickness and a capacitor area range from $7.10 \times 10^{-4} \text{ cm}^2$. The measurements were taken by connecting a Pt bottom electrode to the drive of the precision LC and the Au top electrode to the drive of the precision LC. The P-V hysteresis and J-V characteristics of PZT samples showed the asymmetry for both measurements. The P-V hysteresis loops, J-V and C-V behavior were shifted in the positive direction when the drive was applied to the Pt electrode, while being negatively shifted in the converse case. The asymmetric behavior of the polarized state in the hysteresis loops due to the electrode configuration resulted from different work function between the Pt and Au electrodes, further influencing the leakage current behavior and the capacitance voltage.

Index Terms—PZT films, Pt bottom electrode, Au top electrode, different work function, asymmetries

I. INTRODUCTION

For applications to ferroelectric random access memory (FeRAM), recently, most research studies have been concerned with obtaining high-quality lead zirconate titanate (PZT) films. PZT films are a promising candidate for future FeRAM, which is non-volatile memory that uses ferroelectric material in order to maintain an electric charge [1]. These are due to their excellent properties, such as: high dielectric constants, high remnant polarization and large piezoelectric coefficient. Properties of PZT film depend on many parameters including composition, crystal structure, substrate films, film thickness and electrodes. Concerning the electrodes, it is well known that the bottom and top electrodes have a strong effect on ferroelectric properties. In particular

the bottom electrode plays a critical role in determining the texture and quality of the ferroelectric films, which are closely related to the remanent polarization (P_r).

For electrode materials of PZT thin films in FeRAM, various materials such as platinum (Pt) [9], strontium oxide (SrO) [10], Ru [11, 12], RuO₂ [13], Ir [14], and IrO₂ [15] have been studied. Among them, Pt thin films are widely used as a bottom electrode for PZT capacitor due to numerous characteristics, including low electrical resistivity, large work function, high melting point, high stability in a high-temperature oxidizing atmosphere and high catalytic activity [9]. However, ferroelectric capacitors with catalytic metals (Pt) [16-18] as top electrode are more severely damaged by hydrogen than those with a non-catalytic metal such as Au. The hydrogen-induced degradation would be characterized by a decrease in remanent polarization and an increase in leakage current. While it is not fully understood how this happens, a recent study reported that the aforementioned degradation is significantly affected by the material used as a top electrode. Therefore, gold is chosen to use for an electrical contact of the top electrode due to its resistance to corrosion, electrical conductivity, lack of toxicity and the fact that it is a non-catalytic metal.

Ferroelectric are commonly characterized by a hysteresis loop in the polarization vs. voltage. The characteristic hysteresis loop of PZT films are positively and negatively shifted to $\pm V_c$ or $\pm E_c$ (asymmetry) and exhibits disclosure of the hysteresis loop (a polarization gap between the starting and ending negative voltage leg). However, asymmetric behaviors can be induced by various factors, such as the defect charges present in the ferroelectric material, difference in the work function at the top and bottom electrodes, and interfacial charges [2]. In the present study, a PZT film was deposited on a Pt/Al₂O₃/SiO₂/Si substrate by MOCVD method and circular Au top electrodes with diameters of 300 μm were patterned using a shadow mask by a vacuum evaporation method. The systematic asymmetric hysteresis loop behaviors and relationship with J-V characteristics and C-V characteristics will be described and discussed in this paper.

II. MATERIALS AND METHODS

The substrates used in this work were 8-inch silicon wafers with a platinum bottom electrode layer and an Al₂O₃ adhesion layer. The generated substrate structure was

Masruroh is with Physics Department, Faculty of Mathematics & Natural Science, Brawijaya University, Malang, Indonesia (e-mail:rafizen_02@yahoo.com). Masayuki TODA is with the Department of Chemistry and Chemical Engineering, Yamagata University, Yonezawa-Yamagata 992-8510. WACOM R&D CO., LTD, 568 TANAKA, Fukaya shi, Saitama 369-1108, Japan.

Pt/Al₂O₃/SiO₂/Si(100). The PZT films were grown on the Pt/Al₂O₃/SiO₂/Si(100) substrate using a liquid delivery metal organic chemical vapor deposition (MOCVD) system named "Doctor T" developed by Yamagata University and WACOM R&D Corporation. This MOCVD system features a novel instantaneous vaporizer and has excellent stability for depositing homogeneous films for large wafers. A 90-nm thick film was deposited on the Pt bottom electrode. In the growth of the PZT films, the source precursors used were Pb(DMAMP)₂: 1.570 ccm, Zr(MMP)₄: 0.870 ccm, and T(MMP)₄: 1.460 ccm, and the total pressure was 1067 Pa and the deposition time was 3 min. Oxygen (O₂) and argon (Ar) were used as the oxidizing gas and carrier gas, respectively. The source materials used in this study and typical deposition condition are summarized in Table 1.

TABLE 1 SUMMARY OF PZT DEPOSITION CONDITIONS

Pb sources	1.57 ccm
Ti sources	0.87 ccm
Zr sources	1.46 ccm
Substrate	Pt/Al ₂ O ₃ /SiO ₂ /Si
Thickness of Pt	100 nm
Thickness of Al ₂ O ₃	20 nm
Thickness of SiO ₂	100 nm
Thickness of PZT	90 nm
Carrier gas (Ar) flow rate	1.7 SLM
Oxygen gas flow rate	5 SLM
Suceptor temperature	525 C
Total pressure	1067 Pa
Deposition time	3 min

For electrical characterization of the thin films, gold top electrodes were applied to the film surfaces using a shadow masking evaporation method. The top electrode structures were patterned with circles using a shadow mask with a diameter of 300 μm. The films were annealed by an RTA process at temperature of 580 C for 30 sec in an O₂ atmosphere in order to crystallize the PZT films in the ferroelectric phase. X-ray diffraction (XRD, Rigaku 3272) with CuKα radiation was used to examine the crystal orientation of the PZT films. The composition of the film was measured using X-ray fluorescence (XRF, Rigaku system 3272).

The polarization as a function of voltage (P-V hysteresis), current density as a function of voltage (J-V curve), and capacitance as a function of voltage (C-V curve) were measured after performing a RTA process. A ferroelectric test system (Precision LC Radiant Technology) was used to measure their electrical properties. The sample thickness of PZT was 90-nm and the capacitor area range of 7.10 × 10⁻⁴ cm². Two types of measurements were made in this work: first, the drive terminal bottom electrode (Pt) was connected to the drive of the precision LC (Fig. 1a), and second, the Au top electrode was connected to the drive of the precision LC (Fig. 1b).

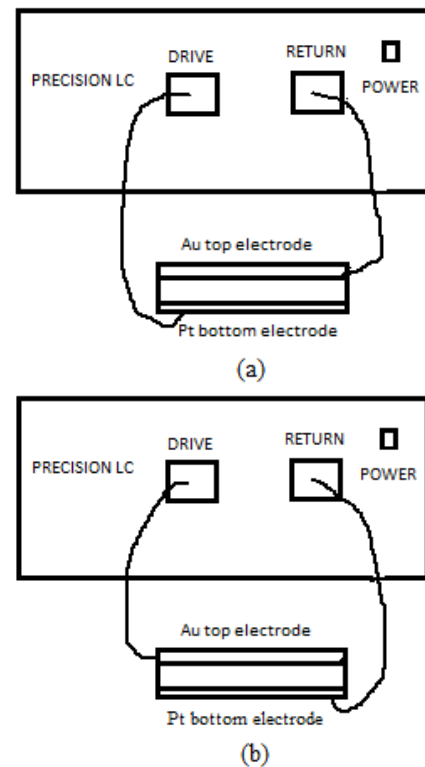


Fig. 1. Illustration model of drive and return port connections to top and bottom electrode of the sample: (a) when drive is applied to Pt electrode, and (b) when drive is applied to Au electrode.

III. RESULTS AND DISCUSSIONS

The chemical composition of the PZT films shows a mol concentration of PbO: 52.272 mol%, ZrO₂: 21.263 mol% and TiO₂: 21.263 mol%, respectively. The summary of PZT composition is shown in Table 2. Figure 2 shows the XRD pattern of the PZT films as deposited and after performing a rapid thermal annealing (RTA) process. The as-deposited PZT films shows no perovskite phase of PZT films, while after RTA process the formation of perovskite phase was occurred. The films show a mixture of PZT (001/100), (111) and (002/200) indicative of being polycrystalline.

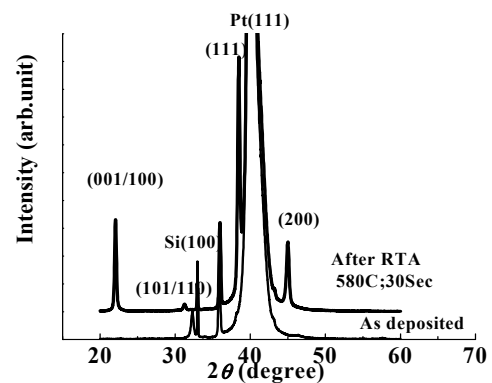


Fig. 2. XRD pattern of the PZT films observed as deposited and after RTA process.

All of the P-V hysteresis loops were measured at a frequency of 1 kHz for the sample with 90-nm PZT thickness and a capacitor area of 7.10 × 10⁻⁴ cm². In Fig. 3, a typical P-V hysteresis loop of the films is shown for a maximum applied voltage of ±5 V. As shown in the figure, the hysteresis loops

show little disclosure and are shifted in the positive direction when the Pt electrode connected to the drive of the precision LC. The results show that the remnant polarization of the positive direction is obviously smaller than that of the negative direction, that is, the remnant polarizations show $Pr_+ \approx 8.441 \mu\text{C}/\text{cm}^2$ and $Pr_- \approx 23.773 \mu\text{C}/\text{cm}^2$. Conversely, as shown in Figure 4, when the Au connected to the precision LC, all of the hysteresis loops show an inverted asymmetric and the gap of the hysteresis loop is obviously larger than that observed when the drive was applied to Pt.

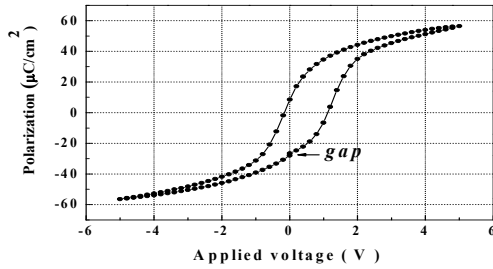


Fig.3. P-V Hysteresis of PZT films at $V_{\text{max}} 5 \text{ V}$; when drive applied to Pt.

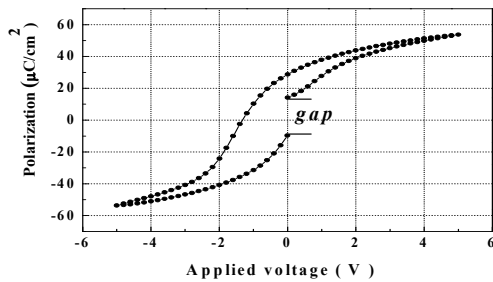


Fig.4. P-V Hysteresis of PZT films at $V_{\text{max}} 5 \text{ V}$; when drive applied to Au.

The hysteresis loop shifted in the negative direction and the remnant polarization of the positive direction is obviously larger than those of the negative direction, that is, the remnant polarizations show $Pr_+ \approx 26.789 \mu\text{C}/\text{cm}^2$ and $Pr_- \approx 14.125 \mu\text{C}/\text{cm}^2$. Furthermore, by applying the drive to Pt, the end point of the loop is below the initial point, conversely, the initial point of the loop is below the endpoint when the drive is applied to Au. This is evident by the fact that the positive half of the loop shows disclosure, such that the lower portion of the legs drops. It should also be noted that based on the above results, the sample may lead to imprint failure caused by unstable positively and negatively poled states, a positive imprint when the drive is applied to the bottom (Pt) electrode and a negative imprint when the drive is applied to the top electrode. The imprint was apparent when the drive voltage was applied to either electrode, but the asymmetry appeared differently, depending on which electrode the drive was applied to. The asymmetries of hysteresis loops in the two opposite directions can be related to the electrode asymmetry (different work function for the bottom and top electrode [2, 3]). Au has a work function of 5.47 eV, whereas the corresponding value for Pt is 5.65 eV. The relationship between the polarization states and different work function in the ferroelectric capacitor can be considered via the model depicted in the Fig. 8. For the case in which, the drive is applied to Au electrode (Fig. 8, right), the drive port provides a positive DC voltage stimulus to the Au electrode, and the

return port reads the sample currents from the Pt electrode. The field shows a switch from the positive polarization state to the negative one. Since the work function of Au is lower than that of Pt ($\Phi_{\text{Au}} < \Phi_{\text{Pt}}$), an electron from the Au electrode is unlikely to move to the Pt electrode, implying that it is more difficult for the system to switch from final negative polarization to the initial positive one. As a result, a large gap occurs between the final polarization and the initial one, as depicted in the Fig. 4. In the converse case as shown in the figure, when the drive is applied to the Pt electrode, because of the work function of Au is lower than that of Pt, it is implied that an electron from Pt can easily move to the Au electrode, thus the gap between the end point of polarization is small.

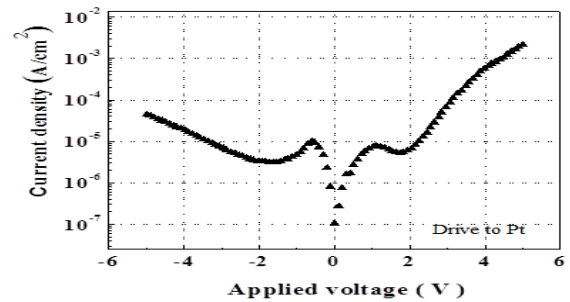


Fig.5. J-V characteristics of PZT films at $V_{\text{max}} 5 \text{ V}$; when drive applied to Pt.

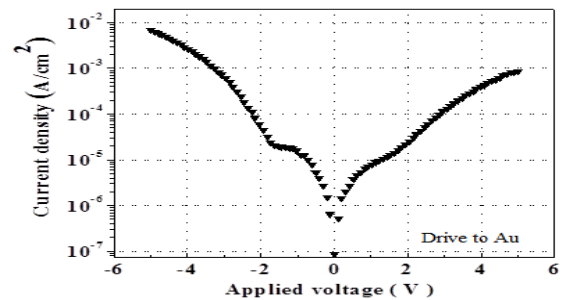


Fig.6. J-V characteristics of PZT films at $V_{\text{max}} 5 \text{ V}$; when drive applied to Au.

Figure 5 and 6 show the J-V characteristics of the samples with different drive port connections to the electrode, which were measured in the voltage range of $\pm 5 \text{ V}$ with a delay time of 100 ms. All of the leakage current densities exhibit asymmetries. The leakage current under a positive bias is higher than that under a negative bias when the drive is applied to Pt bottom electrode, and in the converse case when the drive is applied to Au, the leakage current under a negative bias is higher than that under positive bias. The leakage asymmetry in this case also relates to the different work function of these electrodes. The difference in work functions leads to different height barriers at the bottom and top interfaces between the PZT capacitor [2-5]. The relationship between current density and potential barrier height is given by the following equation [5, 6]:

$$J \sim \exp[-q/kT(\Phi_B^0 - \Delta\Phi)] \quad (1)$$

where Φ_B^0 is the potential at zero applied field and $\Delta\Phi$ is the barrier reduction due to schottky effect, q is the electronic charge, k is the Boltzman constant and T is the absolute

temperature. The $(\Phi_B^\circ - \Delta\Phi)$ difference gives the apparent potential barrier. Equation (1) shows the leakage current density dependent on the potential barrier Φ_B° . In the Schottky theory [6, 8], the height of the potential barrier is simply assumed as the difference between the metal work function Φ_m and the semiconductor (Φ_s) [5]. The work function is the energy difference between vacuum level and Fermi level (E_F). When a forward bias voltage V_a is applied to the junction, the barrier height in the semiconductor becomes $q(\Phi_B - V_a)$ and the electron flow from the semiconductor into the metal is enhanced by a factor, $\exp(V_a/kT)$ [19]. Based on illustration model as shown in Fig. 5 and equation (1) above, it can be assumed that, for the drive applied to Pt, the positive leakage current was limited by the interface between Pt bottom electrode and the PZT film (bottom interface), while the negative leakage current was limited by the interface between Au electrode and the PZT film (top interface). Since the barrier height at the negative bias is higher than at the positive bias, therefore the leakage current under a positive bias can be much higher than that under a negative bias. In the converse case, when drive is applied to Au, the positive leakage current is limited by the Au top electrode and the PZT film (top interface), while the negative leakage current is limited by Pt bottom electrode and PZT film (bottom interface), which has a lower barrier height. Therefore, the leakage current under a negative bias can be much higher than that under a positive bias. In addition, corresponding to the current leakage behavior and the asymmetric hysteresis loop, the capacitance-voltage (C-V) curve is also shifted in the positive direction, when drive is applied to Pt, in the converse case (when drive is applied to Au as shown in Fig. 7, the C-V curve is shifted in the negative direction.

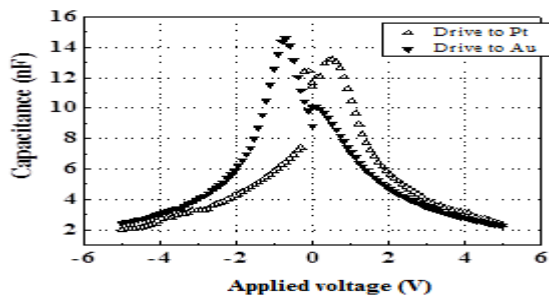


Fig.7. C-V characteristics of PZT film at V_{max} 5 V with a drive was connected to Pt and Au electrode.

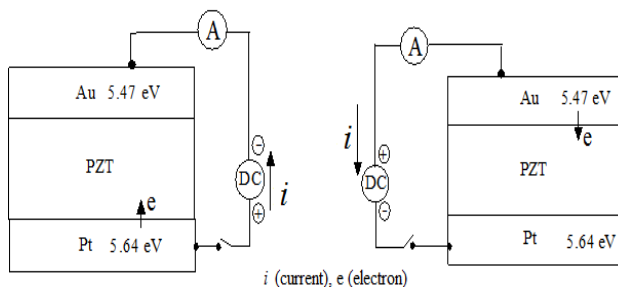


Fig 8. Illustration model of Pt/PZT/Au structure with a different top and bottom electrode and work function; when drive applied to Pt (left) and drive applied to Au (right)

Furthermore, deposition at different temperatures may also lead to the asymmetries, since the Pt bottom electrode is

deposited at a relatively high temperature, while the Au top electrode is deposited at a low temperature. As a result the bottom electrode receives a higher heat burden than does the top electrode. This leads to an increase in the interface state density at the bottom interfaces, as a result, the Schottky barriers at the interfaces of the ferroelectric elements will be asymmetric [7].

TABLE 2 SUMMARY OF PZT COMPOSITION

Chemical structure	Composition
PbO (mol%)	48.7
ZrO2 (mol%)	23.4
TiO2 (mol%)	27.9
Pb/(Zr+Ti)	0.949
Zr/(Zr+Ti)	0.455
Ti/(Zr+Ti)	0.545

TABLE 3 SUMMARY RESULTS OF $\pm V_C$ AND $\pm P_R$ OF THE PZT SAMPLE

Parameter	Drive to Pt	Drive to Au
P_{max} ($\mu C/cm^2$)	47.484	56.613
Pr ($\mu C/cm^2$)	8.441	26.789
-Pr ($\mu C/cm^2$)	-23.773	-14.05
V_c (V)	0.913	0
$-V_c$ (V)	-0.191	-0.854
Offset ($\mu C/cm^2$)	20.405	-1.374

IV. CONCLUSIONS

The P-V hysteresis loops, J-V characteristics and C-V characteristics were investigated on a ferroelectric structure consisting of a platinum bottom electrode, a vapor-deposited gold top electrode and PZT films. The measurements were measured after performing a rapid thermal annealing process using a Precision LC Radiant Technology by applying a drive to the Pt bottom electrode connected to the drive of the precision LC, and on the other hand, the Au top electrode was connected to the drive of the precision LC. The P-V hysteresis, J-V characteristics and C-V characteristics of the PZT samples were asymmetric for both measurements. The asymmetries appeared differently, depending on the electrode to which the drive was applied. When driving the Pt bottom electrode, the polarization shifted in the positive direction, while when the drive was applied to the Au top electrode, the polarization switches shifted in the negative direction. The asymmetries of the hysteresis loops, leakage currents and the capacitance voltage in the two opposite directions were due to the electrode asymmetry in term of the work functions of the Pt bottom electrode and the Au top electrode. In addition, due to their work functions, these electrode materials lead to different barrier height at the bottom and top interfaces, resulting in different leakage currents under a positive and negative bias.

The asymmetries of the hysteresis loops and leakage currents in the two opposite directions were due to the electrode asymmetry in term of the work function of the Pt bottom electrode and the Au top electrode. In addition, due to

their work functions, these electrode materials lead to different barrier height at the bottom and top interfaces, resulting in different leakage currents under a positive and negative bias.

ACKNOWLEDGMENT

The authors are grateful to Mr. Fujimoto and Mr. Kosuke OHNO (from Pioneer) for the annealing PZT sample with RTA and XRD measurements, Mr. Yutaka KOJIMA and Mr. M. OHATA from NFT Co., Ltd, and Mr. Scott. P. Chapman and Mr. Joe T. Evans from Radiant Technologies, Inc. for discussion about Radiant Technologies. The research project was supported by WACOM R&D Co., LTD, 568 Tanaka, Fukaya Shi, Saitama, Japan.

REFERENCES

- [1] J. A. Johnson, J. G. Lisoni and D. J. Wouters, *Microelectronic Engineering*, vol. 70, 2003, pp 377-383.
- [2] C. H. Choi, Jaichan Lee, Bae Ho Park, and Tae Won Noh, *Integrated ferroelectric*, vol 18, 1997, pp. 39-48.
- [3] C. H. Choi and J. Lee, *J. Phys. IV France* vol. 8, 1998, pp. 9-112.
- [4] Raymond T. Tung; "Schottky Barrier Tutorial", Department of Physics, Brooklyn College, CUNY, 2900 Bedford Ave. Brooklyn, NY 11210.
- [5] Lucian Pintilie, Ionela Vrejoiu, Dietrich Hesse and Marin Alexe, *J. Appl. Phys* vol. 104, 2008, pp. 114101.
- [6] W. Schottky, *Phys. Z.* vol. 41, 1940, pp. 570.
- [7] Zheng Lirong, Lin Chenglu, Xu heaping, Zou Shichang and Masanori Okuyama, *Science in China (Series E)*, vol. 40, No.2, 1997, pp. 126-134.
- [8] Sze, S.M. "Physics of Semiconductor Devices 2nd.", John Wiley & Sons, New York, 1981, pp.362-390.
- [9] P. K Bauman, P. Doppelt, K. Frohlich, O. Valet, V. Chambel, D. Machajdik, M. Schumacher, J. Lindner, F. Schienle, H. Guillon and C. Jimenez, "15th International Symposium on Integrated Ferroelectrics (ISIF)", 2003, pp. 392-393.
- [10] Kenji Takahashi, Takahiro Oikawa, Keisuke Saito, Hiriniri Fujisawa, Masaru Shimizu, and Hiroshi Funakabo, *Jpn. J. Appl. Phys.*, 2002, vol. 41, pp. 6873-6876.

- [11] Sang Yeol Kang, Ha Ji Lim, Cheol Seong Hwang and Hyeong Joon Kim, "15th International Symposium on Integrated Ferroelectrics (ISIF)", 2003, pp. 404-405.
- [12] S. D. Berstein, T. Y. Wong, Y. Kisler and R. W. Tustison, *J. Mater. Res.*, 1993, vol. 8, pp. 12.
- [13] H. N. Al. Shareef, A. I. Kingon, X. Chen, K. R. Bellur and O. Auciello: *J. Mater. Res.*, 1994, vol 9, pp. 2968.
- [14] Young Park and Joon Tae Song, *Materials Letters*, 2004, vol. 58, pp 2128-2131.
- [15] K. Okuwada, K. Yoshida, T. Saitou and A. Sawabe, *J. Mater. Res.*, 2000, Vol. 15, pp. 2667.
- [16] June-Mo Koo, Noh-Heon Park, Won Hee Lee, Jae-Gab Lee and Jiyoung Kim, *Journal of the Korean Physical Society*, 2002, vol. 40, no. 4, 729-732.
- [17] Eun Gu Lee, Jay Gab Lee and Sun Jae Kim, *Journal of the Korean Physical Society*, 2006, vol. 48, no. 5, pp. 956-959.
- [18] Jin-Ping and T.P. Ma, *Appl. Phys. Lett.*, 1997, vol. 71, pp. 9.
- [19] Funda Arlaktuturk, Arif Agasiev, Adem Tataroglu, and Semsettin Altindal, G.U., *Journal of Sciences*, 2007, vol. 20 no. 4, pp. 97-102.



Masruroh was born in Jombang-Indonesia, on December 31, 1975, she received Bachelor degree (1999), from Physics Department, Brawijaya University-Malang-Indonesia, Master degree (2002), Physics Department, Institut Teknologi Bandung (ITB)-Indonesia, and D.Eng (2007) from Material Sciences and Energy Engineering, Yamagata University, Japan. She is a lecturer in Physics department, Faculty of Mathematics and Natural Sciences, University of Brawijaya. Her current interests include Ferroelectrics Thin Films, nanotechnology, nano- and micro-manufacturing high dense plasma processing and surface design engineering.

Masayuki TODA, He is a Professor, Department of Chemistry and Chemical Engineering, Yamagata University, 4-3-16 Jonan, Yonezawa, Yamagata 992-0038, Japan, Director WACOM R&D Corporation, 568 Tanaka, Fukaya, Saitama 369-1108, Japan. His current interest includes Ferroelectrics and Piezoelectric Thin Films such as PZT(Lead Zirconate Titanate)